UNIVERSITY OF PATRAS - SCHOOL OF ENGINEERING
DEPARTMENT OF ELECTRICAL AND COMPUTER ENGINEERING

Division: Systems and Automatic Control

Thesis

of the student of the Department of Electrical and Computer Engineering of the School of Engineering of the University of Patras

Karadimos Alexios of Loukas

Student Number: 1046820

Subject

Robotic surgical tool manipulator - Recognition, control and manipulation of laparoscopic tools

Supervisor

Associate Professor Dr. Evangelos Dermatas

Thesis Number:

Patras, 2020

ΠΙΣΤΟΠΟΙΗΣΗ

Πιστοποιείται ότι η διπλωματική εργασία με θέμα

Robotic surgical tool manipulator - Recognition, control and manipulation of laparoscopic tools

του φοιτητή του Τμήματος Ηλεκτρολόγων Μηχανικών και Τεχνολογίας Υπολογιστών

Karadimos Alexios of Loukas

(A.M.: 1046820)

παρουσιάστηκε δημόσια και εξετάστηκε στο τμήμα Ηλεκτρολόγων Μηχανικών και Τεχνολογίας Υπολογιστών στις

__/__/___

Ο Επιβλέπων

Ο Διευθυντής του Τομέα

Evangelos Dermatas
Associate Professor Dr.

Kazakos Demosthenes
Assistant Professor Dr.

Contents

1 Introduction

2 Robotic arm Kinematic Analysis

2.1 Robotic arm, DH parameters & Forward Kinematics

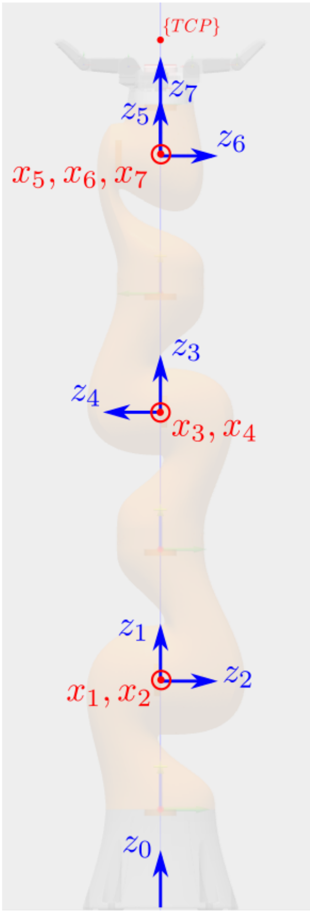

Figure 1: Joint reference frames of the KUKA iiwa14 robot

i	θ_i (rad)	L_{i-1} (m)	d_i (m)	α_{i-1} (rad)
1	θ_1	0	0.36	0
2	θ_2	0	0	$-\pi/2$
3	θ_3	0	0.36	$\pi/2$
4	θ_4	0	0	$\pi/2$
5	θ_5	0	0.4	$-\pi/2$
6	θ_6	0	0	$-\pi/2$
7	θ_7	0	0	$\pi/2$

$$
{}^{i-1}T_i = \begin{bmatrix} c\theta_i & -s\theta_i & 0 & L_{i-1} \\ s\theta_i ca_{i-1} & c\theta_i ca_{i-1} & -sa_{i-1} & -sa_{i-1}d_i \\ s\theta_i sa_{i-1} & c\theta_i sa_{i-1} & ca_{i-1} & ca_{i-1}d_i \\ 0 & 0 & 0 & 1 \end{bmatrix}
$$

2.2 Inverse Kinematics

2.2.1 Decoupling Technique

In this section the inverse kinematics problem is solved for only the 6 out of the 7 total degrees of freedom. The third joint is not used in this analysis and it's angle is set to zero $\theta_3 = 0$. The rest of the joints form a special kind of kinematic chain that can be solved using the decoupling technique. In this technique the Inverse kinematics problem is split to 2 separate subproblems, one for the position and one for the orientation of the end-effector. This technique can be applied in this case because the axes of the 3 last joints intersect at the same point and they form an Euler wrist.

To solve for the joints' angles, the transformation matrix ${}^0T_7$ of the end-effector with respect to the robot's base is required. Usually the transformation ${}^UT_{tcp}$ is known, which is the pose of Tool's center point (TCP) with respect to the Universal Coordinate Frame $\{U\}$ from which the required ${}^0T_7$ can be calculated

$$
\begin{gathered}
{}^UT_{tcp} = {}^UT_0 \; {}^0T_7 \; {}^7T_{tcp} \\
{}^0T_7 = {}^UT_0^{-1} \; {}^UT_{tcp} \; {}^7T_{tcp}^{-1} \\
{}^0T_7 = \begin{bmatrix} R_t & \mathbf{p}_t \\ 0 & 1 \end{bmatrix}
\end{gathered}
$$

where ${}^UT_0, \;\; {}^7T_{tcp}$ are translation transformations by a constant distance and $R_t, \;\; \mathbf{p}_t$ are the target's orientation and position respectively.

$$
{}^0\mathbf{p}_5 = {}^0T_4 {}^4\mathbf{p}_5 = \begin{bmatrix} p_x \\ p_y \\ p_z \end{bmatrix}
$$

$$
\theta_1 = \begin{cases} atan2\left(p_y, p_x\right) \\ \pi - atan2\left(p_y, p_x\right) \end{cases} \tag{2.2.1}
$$

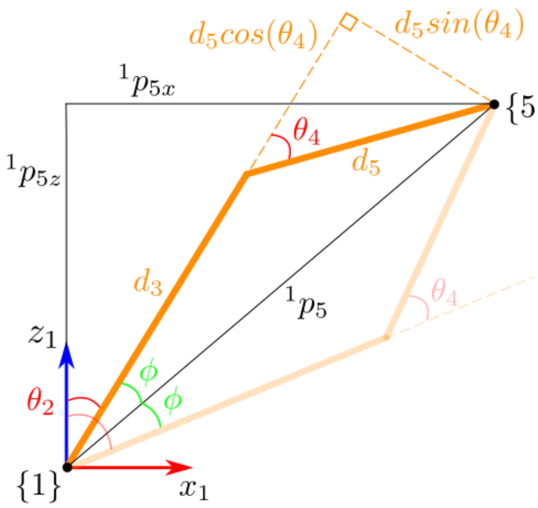

Figure 2: Calculation of angles θ_2, θ_4

$$
\varphi = acos\left(\frac{d_3^2 + \|{}^1p_5\|^2 - d_5^2}{2d_3\|{}^1p_5\|}\right)
$$

$$\theta_2 = atan2\left(\sqrt{p_x^2 + p_y^2}, {}^1p_{5z}\right) \pm \varphi \tag{2.2.2}$$

$$c_4 = \frac{\|{}^1p_5\|^2 - d_3^2 - d_5^2}{2d_3d_5}$$

$$\theta_4 = atan2\left(\pm\sqrt{1 - c_4^2}, c_4\right) \tag{2.2.3}$$

Once $\theta_1, \theta_2, \theta_3, \theta_4$ are known, the orientation matrix of the wrist can be calculated as following

$$R_{target} = \begin{bmatrix} i_x & j_x & k_x \\ i_y & j_y & k_y \\ i_z & j_z & k_z \end{bmatrix}$$

$$\theta_6 = atan2\left(\pm\sqrt{1 - k_y^2}, k_y\right) \tag{2.2.4}$$

$$\theta_7 = atan2\left(-j_y, i_y\right)$$

$$\theta_5 = atan2\left(-k_z, k_x\right)$$

2.2.2 Workspace constraints & Singularity points

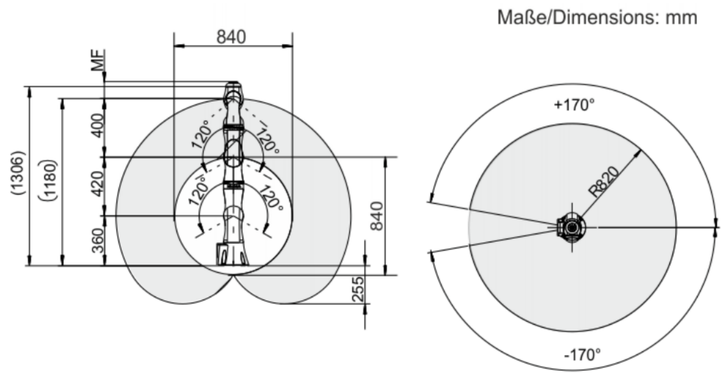

Figure 3: KUKA iiwa LBR14 workspace dimensions

Singularity points:

- When $p_x^2 + p_y^2 = 0$ then the end-effector lies on the z-axis and θ_1 is not defined
- When $sin\left(\theta_6\right) = 0$ then the angles θ_5, θ_7 are not defined

2.2.3 Solutions for 7DoF numerically

2.2.4 Comparison of Inverse Kinematics Techniques

3 Grasping

3.1 Gripper & Forward Kinematics

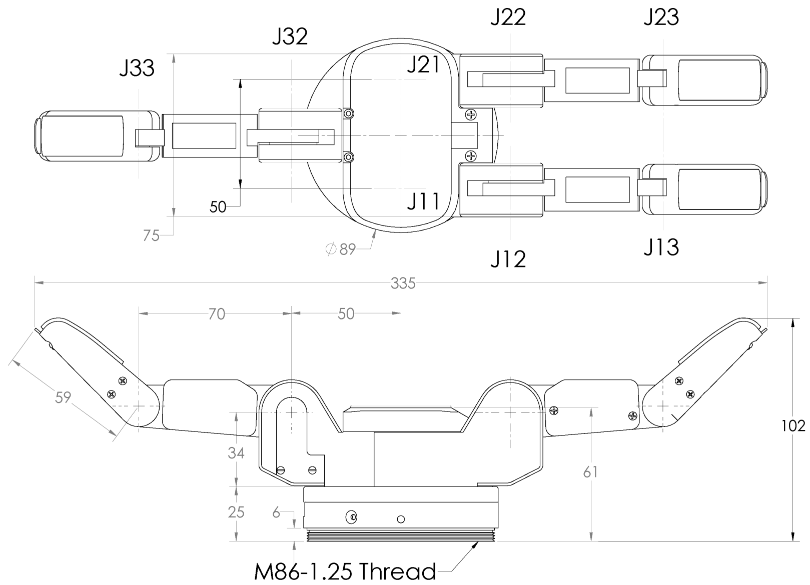

Figure 4: Barrett Hand gripper (model BH8-282) dimensions

3.2 Gripper Inverse Kinematics

The following Inverse Kinematics analysis referes to one finger of the Barrett Hand gripper, which has 3 revolute joints. Finger 3 has only 2 revolute joints for which the angle solutions are the same with the solutions of the last 2 joints of the other fingers. Let

$$\mathbf{p} = \begin{bmatrix} p_x \\ p_y \\ p_z \end{bmatrix}$$

be the position of the grasp point for one finger. The first angle can easily be calculated as

$$\varphi_1 = atan2\left(p_y, p_x\right) \tag{3.2.1}$$

Next, we calculate the third angle based on the law of cosines (see fig.)

$$cos\left(\pi - \varphi_3 - \frac{\pi}{4}\right) = \frac{L_2^2 + L_3^2 - p^2}{2L_2L_3}$$

$$cos\left(\varphi_3 + \frac{\pi}{4}\right) = \frac{p^2 - L_2^2 - L_3^2}{2L_2L_3}$$

$$\varphi_3 = atan2\left[\pm\sqrt{1 - \left(\frac{p^2 - L_2^2 - L_3^2}{2L_2L_3}\right)^2}, \frac{p^2 - L_2^2 - L_3^2}{2L_2L_3}\right] - \frac{\pi}{4} \tag{3.2.2}$$

In a more general case, the first argument of the $atan2$ function in the expression of φ_3 could also be negative, but in this case this second solution is rejected, because due to mechanical constraints, this angle can't be negative. After having calculated φ_3 we can calculate φ_2

$$tan\left(\psi+\varphi_2\right)=\frac{p_z}{\sqrt{p_x^2+p_y^2}}$$

$$tan\left(\psi\right)=\frac{L_3 sin\left(\varphi_3+\frac{\pi}{4}\right)}{L_2+L_3 cos\left(\varphi_3+\frac{\pi}{4}\right)}$$

$$\varphi_2=atan2\left(pz,\sqrt{p_x^2+p_y^2}\right)-atan2\left[L_3 sin\left(\varphi_3+\frac{\pi}{4}\right),L_2+L_3 cos\left(\varphi_3+\frac{\pi}{4}\right)\right] \tag{3.2.3}$$

3.3 Force closure

The planar case, the spatial case & convex hull test.

3.4 Firm grasping algorithm & Force control

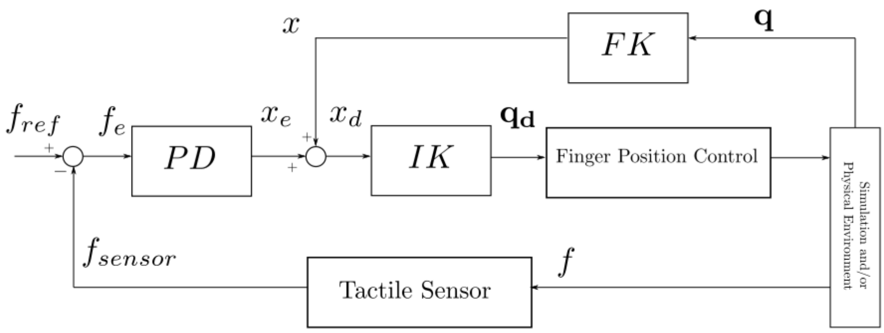

Figure 5: Force control on a Barrett Hand gripper finger

4 Scene and object recognition with Computer Vision

4.1 Laparoscopic tool detection

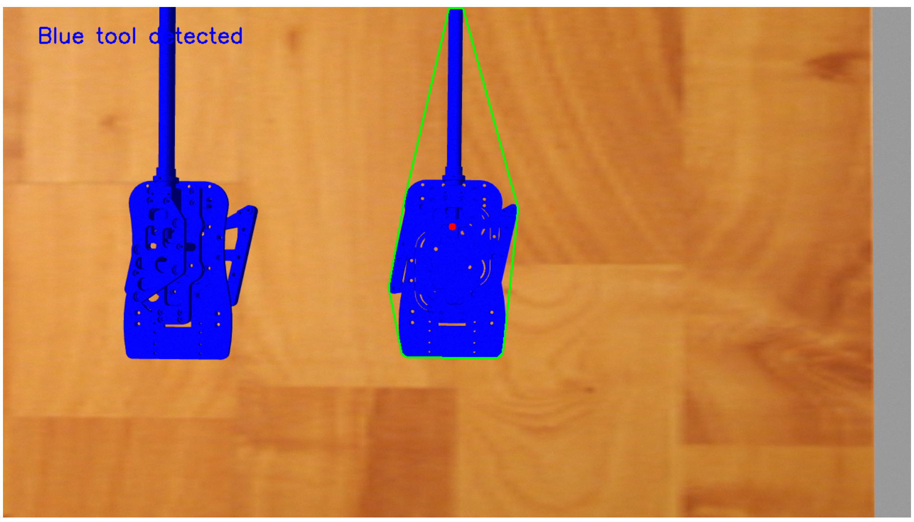

Figure 6: Simple tool detection in simulation based on color, using OpenCV. The green polygon is the convex hull, and the red point is the estimated center of mass

4.2 Calculation of tool position and orientation

In order for the gripper to grasp correctly the laparoscopic tool, it is required to calculate the tool's position and orientation in the pixel space which must then be converted with respect to the robot's workspace. From all the pixels that have been classified as part of the laparoscopic tool, one can estimate the center of mass and two perpendicular vectors attached to that point that define the orientation. The center of mass is simply the average of the (x, y) coordinates of all the tool's pixels

$$(\bar{x}, \bar{y}) = \left(\frac{1}{N} \sum_{i=1}^{N} x_i, \frac{1}{N} \sum_{i=1}^{N} y_i \right)$$

The two orientation vectors are the eigenvectors of the covariance matrix of the above pixels. Let $\mathbf{a}, \mathbf{b}$ be the orientation vectors, then $\mathbf{a}, \mathbf{b}$ are solutions of the equation

$$C\mathbf{v} = \lambda \mathbf{v}$$

where C is the covariance matrix given by

$$C = \begin{bmatrix} \sigma(x, x) & \sigma(x, y) \\ \sigma(y, x) & \sigma(y, y) \end{bmatrix}$$

$$\sigma(x, y) = \frac{1}{n-1} \sum_{i=1}^{N} (x_i - \bar{x})(y_i - \bar{y})$$

4.3 Calculation of grasping points

4.4 Trocar detection & Estimation of fulcrum point

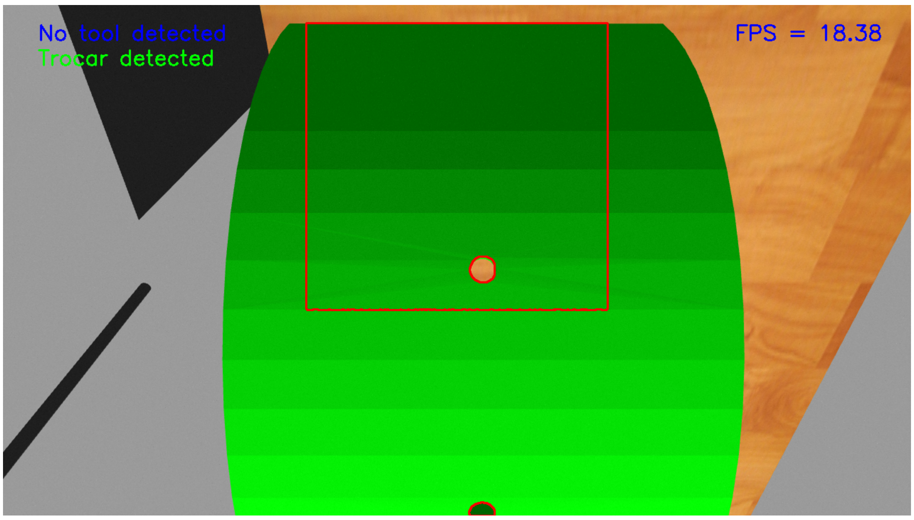

Figure 7: Simple trocar detection in simulation based on color, using OpenCV. In simulation, the trocar is simply considered to be a small cylindrical hole and it's center is the fulcrum point

5 Laparoscopic tool manipulation

5.1 Pivoting motion with respect to Fulcrum Point

6 Path Planning

6.1 Path searching

Find path points (position and orientation) by avoiding collisions, asserting that path points is within robot's workspace and by avoiding singularity points.

6.2 Pick and place algorithm

7 Trajectory Planning

7.1 Trajectory planning in cartesian coordinates

Connect the points from path planning with line segments and add more points if needed

7.2 Trajectory planning in joint angles space

8 Simulation with the ROS framework

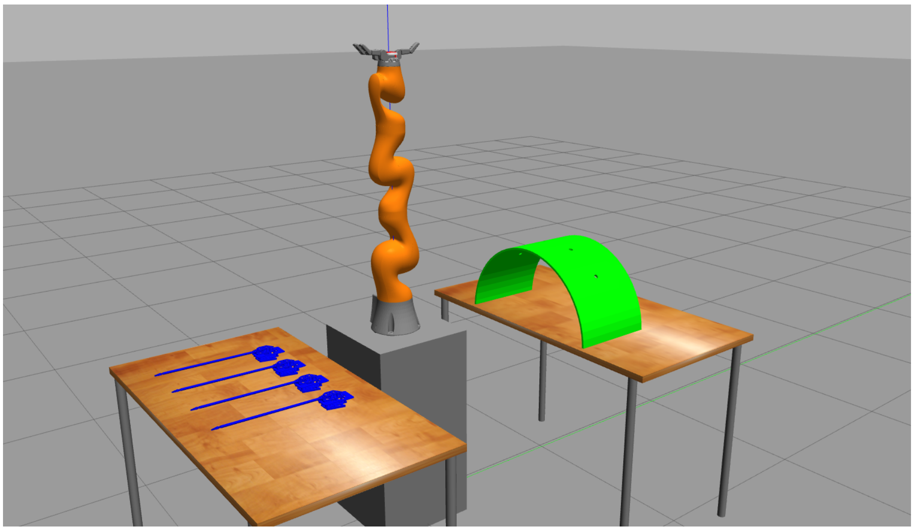

Figure 8: Simulation environment in Gazebo

Nomenclature

${}^{i-1}\mathbf{p}_{iO}$ Position vector from the origin of the coordinate frame $\{i\}$ to the origin of the coordinate frame $\{i-1\}$

${}^{i-1}R_i$ Rotation matrix from coordinate frame $\{i\}$ to coordinate frame $\{i-1\}$

${}^{i-1}T_i$ Transformation matrix from coordinate frame $\{i\}$ to coordinate frame $\{i-1\}$

c_i Shorthand notation for $cos\theta_i$

$J^\dagger$ Geometric Jacobian or the Pseudoinverse of the Jacobian

s_i Shorthand notation for $sin\theta_i$

List of Figures

List of programs

Bibliography

[1] Sachin Chitta et al. "ros_control: A generic and simple control framework for ROS". In: *The Journal of Open Source Software* (2017). DOI: 10.21105/joss.00456. URL: http://www.theoj.org/joss-papers/joss.00456/10.21105.joss.00456.pdf.

[2] Carlos Faria et al. "Position-based kinematics for 7-DoF serial manipulators with global configuration control, joint limit and singularity avoidance". In: *Mechanism and Machine Theory* 121 (2018), pp. 317–334. ISSN: 0094-114X. DOI: https://doi.org/10.1016/j.mechmachtheory.2017.10.025. URL: http://www.sciencedirect.com/science/article/pii/S0094114X17306559.

[3] Carlos Faria et al. "Position-based kinematics for 7-DoF serial manipulators with global configuration control, joint limit and singularity avoidance". In: *Mechanism and Machine Theory* 121 (Mar. 2018), pp. 317–334. DOI: 10.1016/j.mechmachtheory.2017.10.025.

[4] M. R. Hasan et al. "Modelling and Control of the Barrett Hand for Grasping". In: *2013 UKSim 15th International Conference on Computer Modelling and Simulation*. Apr. 2013, pp. 230–235. DOI: 10.1109/UKSim.2013.142.

[5] Felix C. Huang et al. "Learning kinematic mappings in laparoscopic surgery". In: *Conference proceedings : ... Annual International Conference of the IEEE Engineering in Medicine and Biology Society. IEEE Engineering in Medicine and Biology Society. Annual Conference* 2010 (2010). PMC3280950[pmcid], pp. 2097–2102. ISSN: 1557-170X. DOI: 10.1109/IEMBS.2010.5626188. URL: https://pubmed.ncbi.nlm.nih.gov/21095685.

[6] Reza N. Jazar. *Theory of Applied Robotics, Kinematics, Dynamics, and Control (2nd Edition)*. Springer, Boston, MA, 2010. ISBN: 978-1-4419-1750-8. DOI: 10.1007/978-1-4419-1750-8.

[7] I. Kuhlemann et al. "Robust inverse kinematics by configuration control for redundant manipulators with seven DoF". In: *2016 2nd International Conference on Control, Automation and Robotics (ICCAR)*. Apr. 2016, pp. 49–55. DOI: 10.1109/ICCAR.2016.7486697.

[8] Kevin M Lynch and Frank C. Park. *Modern Robotics: Mechanics, Planning, and Control*. English (US). Cambridge Univeristy Press, 2017. ISBN: 978-1107156302.

[9] Victor F. Muñoz et al. "Pivoting motion control for a laparoscopic assistant robot and human clinical trials". In: *Advanced Robotics* 19 (2005), pp. 694–712.

[10] Haiwang Xu et al. "Laparoscopic Robot Design and Kinematic Validation". In: Jan. 2007, pp. 1426–1431. DOI: 10.1109/ROBIO.2006.340138.

[11] Tao Yang et al. "Mechanism of a Learning Robot Manipulator for Laparoscopic Surgical Training". In: *Intelligent Autonomous Systems 12*. Ed. by Sukhan Lee et al. Berlin, Heidelberg: Springer Berlin Heidelberg, 2013, pp. 17–26. ISBN: 978-3-642-33932-5.